JOURNAL OF Materials CHEMISTRY

Formation of a strong, high-porosity spinodal silica and its impregnation with a perfluoro ionomer to obtain a high performance solid acid catalyst composite

Kazuo Okuyama

Ion Exchange Membrane Technology Development Dept., Asahi Chemical Industry Co., Ltd., 1-3-1 Yako, Kawasaki-ku, Kawasaki-shi, 210-0863, Japan

Received 6th December 1999, Accepted 12th January 2000
Published on the Web 29th February 2000

Spinodal silicas, with similar properties to phase-separated glasses but showing high mechanical strength, with large pore sizes and porosities (total pore volume to total particle volume) of 0.7 or more have been produced by adding monobasic sodium phosphate and ammonium molybdate to a silica sol, drying to obtain particles, baking at about 700 °C, and washing in hot water. The porosity was governed mainly by the monobasic sodium phosphate and ammonium molybdate addition, and the microstructure and pore size by the baking temperature and time, with short low-temperature baking yielding a spheroidal silica similar in properties to silica gels and high-temperature baking resulting in the spinodal microstructure. Spinodal silica particles of 1.1 μm average pore size and 0.74 porosity were filled with perfluoro ionomer solution and heat treated at 250 °C after solvent removal, to obtain composite particles of 0.7 μm average pore size and 0.51 meq g^{-1} exchange capacity. The composite particles exhibited high mechanical strength and resistance to chemical desorption of the perfluoro ionomer, and strong catalytic activity as shown by the reaction rate constant of 0.98 L mol^{-1} min^{-1} $eq(H^+)^{-1}$ for the synthesis of ethyl acetate at 60 °C and ambient pressure, which was 1.4 to several times the rate obtained under the same conditions with commercially available catalysts.

Introduction

Porous silicas are typically composed of (1) silica gels formed from silane monomer solutions under controlled acidity,[1] (2) porous glasses (phase-separated glasses) such as borosilicate glass[2] or shirasu porous glass[3] formed by phase separation, and (3) sintered glasses formed by sintering silica particles. Porous glasses are commonly used for liquid filtration and more recently for emulsion production.[4] More generally, porous silicas are used as catalyst or adsorbent carriers, in which the pore requirements differ substantially with the application.

In silica gels, the average pore size is generally small, and the pore-size distribution is large. They are relatively low in mechanical strength, because of their spheroidal particle structure, and their maximum porosity (ratio of total pore volume to total gel volume) is therefore about 0.6. Phase-separated glasses, on the other hand, generally show a sharp pore-size distribution, permit fairly close control in a large range of average pore sizes, and provide relatively high mechanical strength because of their spinodal structure. Their maximum porosity, however, is generally limited to about 0.55,[3] because of constraints imposed on the selection of constituent materials which exhibit phase separation appropriate for formation of the spinodal structure. Sintered glasses generally have a spheroidal microstructure, because of the strong tendency for the area of contact between their constituent silica particles to grow under sintering, and are therefore relatively low in mechanical strength. In short, silica gels and sintered glasses are generally limited in mechanical strength, and phase-separated glasses are inherently limited in maximum porosity.

As described here, we have developed an alternative method of silica particle preparation specifically to avoid these limitations and obtain a mechanically strong, high-porosity silica with macropores (*i.e.*, pores 0.1 μm or more in diameter) of uniform size, similar in structure to phase-separated glasses obtained from the interspacing of salt and glass under spinodal decomposition but formed by a substantially different mechanism, and we have investigated the suitability of the resulting silica for impregnation with perfluoro ionomer to obtain a solid acid catalyst.

Solid acid catalysts have been a subject of widespread and growing interest in recent years, because of problems associated with the use of conventional mineral acids and organic acids as catalysts for organic chemical reactions, including equipment corrosion, difficulty of separation from reaction products and byproducts, and impracticability of regeneration and recycling. Various solid acid catalysts have been proposed, in the form of acidic resins such as perfluoro ionomer acid,[5] phosphorus tungsten acid,[6] and high surface area heterogeneous sulfonic acid,[7] and composites of such an acidic resin with porous silica.

Among solid acid catalysts, fluorides are of particular interest. The strong electronegativity of the fluorine atom and the very small size of its nucleus tend to result in finely structured compounds with high chemical and thermal resistance. If the fluoride contains carboxyl or sulfonic groups, it generally exhibits strong acidity. The catalytic effect of such fluoride containing ionomers has been demonstrated in studies using millimeter sized beads of Nafion,† the perfluorosulfonic acid resin manufactured by Du Pont.[5] In the bead form, however, the surface area is 0.02 m^2 g^{-1} or less and most of the sulfonic groups are located internally, which limits their accessibility and thus their catalytic activity.[8]

To increase the accessibility of the functional groups, composite particles consisting of a porous silica network with entrapped Nafion nanoparticles have been produced by a sol–gel technique involving the hydrolysis and condensation of alkoxysilane mixed with a Nafion solution. The resulting composite particles reportedly show strong catalytic activity, and freedom from ionomer desorption during their use in catalyzing various reactions.[8]

†Nafion is a registered trademark of E. I. Du Pont de Nemours & Co.

DOI: 10.1039/a909620e

With composite particles produced by sol–gel chemistry, however, the possibility exists that significant ionomer desorption may be encountered during the use of the particles for catalysis involving the entry of polar organic solvents into the particles. In addition, production of the composite by the sol–gel technique inherently tends to limit the pore size of the composite, to about 60 nm or less. During the process, the pores are formed when first alcohol, as a product of water hydrolysis, and then water, as a product of condensation reaction, are expelled from the gel.[8] The resulting pores, while large enough to permit movement of the reaction materials and products through the pores during the use of the composite particles in catalysis, may nevertheless limit the speed of this movement and thus limit the overall efficiency of the target reaction. It is possible to obtain larger pores (up to about 500 nm), together with those formed by egressing alcohol and water, by adding $CaCO_3$ powder to the sol, as the $CaCO_3$ dissolves as the gel forms and then egresses from the gel.[8] With this technique, however, it is presumably difficult to obtain a uniform particle-size distribution. Other difficulties may hinder the practical utilization of composite particles obtained by the sol–gel technique. Silica networks obtained by this technique generally consist of spheroidal silica microparticles, and their physical strength is therefore limited. For practical use, moreover, the composite particles must be crushed or otherwise broken into smaller, irregularly shaped particles, which may be susceptible to fragmentation under packing and use in the reaction column, and thus to catalyst loss and clogging of lines and equipment.

Here we describe our investigation on the formation of a solid acid composite by impregnation and heat treatment of the high-porosity spinodal silica particles with perfluoro ionomer, in an attempt to obtain the inherent strength and porosity of the spinodal silica together with the chemical and heat resistance of the perfluoro ionomer, and thus the potential for a broad range of ion-exchange, catalytic, and metal-adsorption capacities based on appropriate selection of the ionomer's functional groups.

Materials and methods

Selection of salt additives for spinodal structure

Various porous silicas were prepared, essentially by mixing a silica sol with one or more inorganic salts (Table 1), baking to obtain the desired silica structure, and removing the salts in hot water.

The starting materials were: silica sol (Snowtex N30, industrial grade; Nissan Chemical Ind., Ltd.) as the silica source material; and sodium dihydrogenphosphate, calcium dihydrogendiphosphate, potassium sulfate, sodium chloride, potassium chloride, calcium chloride, and ammonium molybdate as inorganic salts (all special reagent grades, used without further purification).

A uniform aqueous solution was obtained by adding 100 g of silica sol and 15 g of concentrated nitric acid (special grade; Wako Pure Chemical Ind. Ltd.) to 150 g of water under agitation at room temperature, and further adding one or more inorganic salts in measured amounts under agitation. The solution was then poured onto a steel plate pre-heated to 250 °C and stirred to remove the water by evaporation and obtain dry particles. After baking in an electric oven at 650 °C and 700 °C for 2 h, the particles were placed in 200 mL of water under agitation at 80 °C for 1 h, to elute the organic salts. The elution was performed twice more, and the resulting porous silica was dried by heating to 100 °C for 5 h.

Table 1 Salts used singly or in combination, and the structure of the resulting silica

Salts	Silica structure
NaH_2PO_4	Spheroidal
$NaH_2PO_4 + CaH_2O_7P_2$	Spheroidal
$K_2SO_4 + NaCl$	Spheroidal
$KCl + CaCl_2$	Spinodal
KCl	Spherical
$3(NH_4)_2O{\cdot}7MoO_3 + NaH_2PO_4$	Spinodal

The surface of the porous silica was observed under a scanning electron microscope (S-900; Hitachi, Ltd.), as the basis for determination of spheroidal and spinodal silica structures.

Effect of baking conditions on pore structure

Solutions of the silica sol with inorganic salts in the same compositions which, as described above, had resulted in spinodal porous silica were fed into a spray drier (OC-16; Ohkawara Kakohki Co., Ltd.) at 230 °C to obtain dry particles, which were then baked in an electric oven at 625 °C to 700 °C for 1 h to 2 h. The resulting powders were washed with water and dried in the same manner as described above for the porous silicas, and then observed under the same scanning electron microscope (SEM).

Thermal characteristics of inorganic salts

The thermal characteristics of the inorganic salts which had resulted in spinodal porous silica were determined by thermogravimetric analysis and differential scanning calorimetry (DSC 210; Seiko Instruments) in air with 5 °C min^{-1} as the rate of temperature increase.

Composition of porous silica

A 50 mg sample of the porous silica was carefully weighed in a platinum dish, 3 g of potassium sodium carbonate (special reagent grade; Wako Pure Chemical Ind., Ltd.) and 1 g of sodium borate (special reagent grade; Wako Pure Chemical Ind., Ltd.) were added, and the sample was dissolved by heating over a burner. Next, 15 mL of 6 M hydrochloric acid (Wako Pure Chemical Ind., Ltd.) was added and the contents of the dish were brought to the boil over a heating element, and then brought to 250 mL by adding pure water, followed by ten-fold dilution and then by assay on an induced coupled plasma luminescence analyzer (IRIS-AP; Thermo Jarrell Ash).

Mechanical strength of porous silica

The mechanical strength of each porous silica was measured on a compressive strength tester (MCTM/MCTE; Shimazu Co.).

Preparation of composite particles

From the spinodal porous silica particles with an average pore size of 1.1 μm and a porosity of 0.74, 20 g were taken and placed in a flask equipped with a rotary evaporator, and the pressure in the flask was reduced for 25 min by aspiration. The valve between the evaporator and the aspirator was then closed, and 19.8 g of an aqueous methanol solution of perfluoro ionomer resin (Aciplex; Asahi Chemical Ind. Co., Ltd., Tokyo) (5 wt% resin; methanol/water = 50/50 by weight) was drawn into the flask by the pressure differential. With the flask still under reduced pressure, it was rotated gently on the rotary evaporator for 20 min, to impregnate the silica particles with the solution. The flask was next heated in a water bath, and the methanol/water solvent was removed by pressure reduction and evaporation from the flask. The procedure was repeated a number of times, to obtain impregnated silica particles having the desired resin content.

The impregnated silica particles were placed in an aqueous solution containing a 5 wt% excess of sodium chloride (Wako Pure Chemical Ind., Ltd., special grade) and held at room

temperature for 2 h. They were then filtered and dried, thus obtaining particles impregnated with the perfluoro ionomer in the sulfonic soda state. Next, they were heat treated in an oven at 250 °C in air for 1 h, allowed to cool to room temperature, placed in an excess of 1 M HCl at room temperature for 1 h, and then washed in water to obtain the composite particles, consisting of silica impregnated with the perfluoro ionomer in the sulfonic acid state.

Determination of physical and chemical properties

Porosity (α). The specific weights (d/g ml^{-1}) of the porous silica and composite particles were determined on a density meter (Multivolume Density Meter 1305; Micrometrics Co., Ltd.) using helium gas as the pore filling medium. The unit pore volumes of the particles (ϕ) were determined on a mercury porosimeter (Poremaster-60; Quantachrome). The porosities (α) were calculated from the measured values, according to:

$$\alpha = d\phi/(1+\phi) \quad (1)$$

Pore size. Pore sizes were determined by injection of mercury at pressures of 0.1 to 200 MPa on the above porosimeter, permitting measurements of pores 3.7 to 7500 mm in diameter.

Microstructures. The microstructures of the porous silica and composite particles were observed with a scanning electron microscope (S-800; Hitachi, Ltd.).

Ion exchange capacity. The composite particles were placed in a special column, consisting of a glass cylinder (10 mm diameter, 100 mm length) with a 3G glass filter inserted at the bottom, and 1 M HCl was fed through the column for conversion of the functional groups to sulfonic acid followed by a methanol feed to extract the HCl from the voids until the emerging methanol was confirmed to be neutral by litmus paper testing. Next, aqueous 5 wt% sodium chloride was fed through the column for conversion to the sulfonic sodium state, with titration of the emerging solution for HCl using an aqueous solution of 0.1 M sodium hydroxide. In the final step, first 0.1 M HCl and then methanol was fed through the column for conversion of the functional groups to sulfonic acid, and the particles were then dried. The ion exchange capacity (EC) of the composite was calculated from the weight of the particles after drying (A/g) and the HCl quantity was determined by titration (B/mmol), by the following equation:

$$\mathrm{EC} = B/A \quad (2)$$

Desorption resistance. The resistance of the perfluoro ionomer to desorption from the silica microstructure was evaluated by placing 1 g of the composite particles in 100 g of dimethyl sulfoxide (reagent grade; Wako Pure Chemical Ind., Ltd.) at 90 °C for 3 h, filtering off the dimethyl oxide, washing the particles in fresh dimethyl sulfoxide, and drying the particles, and comparing the ion exchange capacity of the particles before (D/meq g^{-1}) and after (E/meq g^{-1}) this procedure. The percentage of ionomer eluted (R (%)) was calculated as

$$R = (D-E)\times 100/D \quad (3)$$

Determination of catalytic activity

Acetic acid (30.0 g) and ethyl alcohol (23.0 g) (both reagent grade, Wako Pure Chemical Ind., Ltd.) were added to a beaker and stirred to obtain a uniform solution, which was then transferred to a 200 mL three-necked flask equipped with a water-cooled condensor and a Teflon impeller. The catalyst particles (1.00 g) were then added, and the reaction was allowed to proceed under stirring in a water bath at 60 °C, with solution samples (0.20 mL) taken from the flask periodically. Each sample was neutralized by first adding water (10 mL) and several drops of phenolphthalein (reagent grade, Wako Pure Chemical Ind., Ltd.) and then titrating with aqueous 1 M sodium hydroxide (titration grade, Wako Pure Chemical Ind., Ltd.). The acetic acid concentration (F/mol L^{-1}) of each sample was calculated from the titration volume (D_1/mL), by the equation

$$F = 0.1\times D_1\times 10^{-3}/(0.2\times 10^{-3}) \quad (4)$$

The reaction rate constant (k_1/L mol^{-1} min^{-1}) was calculated by using eqn. (5), and the unit reaction rate constant (K/L mol^{-1} min^{-1} eq(H$^+$)$^{-1}$) by using eqn. (6),

$$k_1 = \left[\frac{\sqrt{k_c}}{2F_o}\ln\left|\frac{G-\frac{F_o(k_c+\sqrt{k_c})}{k_c-1}}{G-\frac{F_o(k_c-\sqrt{k_c})}{k_c-1}}\right| - 0.1294\right]/t \quad (5)$$

$$K = k_1/\mathrm{EC} \quad (6)$$

where k_c is the equilibrium constant, which may be expressed by eqn. (7) when the reaction has reached equilibrium and the component concentrations are thus stable,

$$k_c = G^2/F^2 \quad (7)$$

and where F_o is the initial concentration of acetic acid (mol L^{-1}), G is the concentration of ethyl acetate (mol L^{-1}) at equilibrium, and EC is the exchange capacity of the catalyst (eq g^{-1}).

Results and discussion

Inorganic salt additives yielding spinodal silica structure

The salts and salt combinations which were added to the silica sol are shown in Table 1, together with the resulting silica structures. In each case, the quantity of salt added equalled the total pore volume represented by a porosity of 0.65 in the resulting silica, calculated on the assumption that the salts would completely fill all of the pores. It was expected that salts such as monobasic sodium phosphate, calcium dihydrogen pyrophosphate, and ammonium molybdate might tend to form oxidation products under baking in air, and thus contribute to the formation of a spinodal structure. In the event, the salt compositions which yielded this structure, as shown in Table 1, were the combination of potassium chloride and sodium chloride and the combination of ammonium molybdate and monobasic sodium phosphate. Typical electron micrographs of the spinodal and spheroidal structures which were obtained are shown in Fig. 1.

During the baking process, the combination of potassium chloride and sodium chloride resulted in the formation of hydrochloric acid which, among other problems, would have been highly corrosive to the electric oven components. It was therefore eliminated from further consideration in this study, and the ammonium molybdate–monobasic sodium phosphate combination (hereinafter, "molybdate–phosphate salts") thus became the focus of the investigation.

Effect of baking conditions on porous silica structure

Fig. 2 shows the effect of the baking temperature and time on the average pore size and porous structure of silicas which all had a porosity of 0.74 and were obtained by baking spray-dried particles formed from the same composition of silica sol and molybdate–phosphate salts. As shown, the average pore size increased with increasing baking temperature and with increasing baking time, in some cases to more than 2.0 μm. Fig. 2 also shows the region for formation of spinodal structures, as observed by SEM, which occurred with baking temperatures of 675 °C or more in silica with average pore sizes

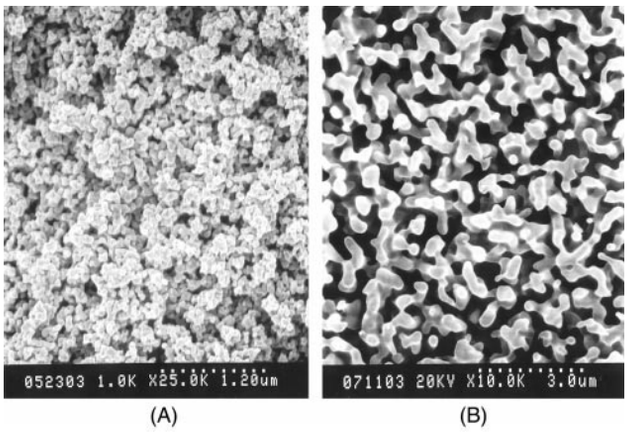

Fig. 1 Scanning electron micrographs of: (A) spheroidal silica structure (× 25 000); (B) spinodal silica structure (× 10 000).

of 0.8 μm or higher. The silica structure was spheroidal at low baking temperatures and short baking times, but the spinodal structure became increasingly evident with either increased baking temperatures or prolonged baking times.

Fig. 3 shows the mercury intrusion curves of three of these silicas. The intrusion peaks occurred at 0.01, 0.2, and 0.8 μm, for silicas baked at 350 °C for 1 h, 750 °C for 15 min, and 750 °C for 1 h, respectively, and sharpened with increasing baking time and temperature.

Although not shown here, spinodal silicas with porosities of 0.85 or higher were also obtained, by further increasing the proportion of salts in the salt and silica sol mixture.

Thermal characteristics of salts

Differential scanning calorimetry (DSC) and thermogravimetric analysis (TG) were performed for powders obtained from the mixture of silica sol, monobasic sodium phosphate and ammonium molybdate (SS–MSP–AM) and from the mixture of monobasic sodium phosphate and ammonium molybdate (MSP–AM) without silica sol. As shown in Fig. 4, the SS–MSP–AM powder exhibited heat absorption troughs at about 100 °C, 310 °C, 335 °C, 610 °C, and 660 °C. The DTA and TGA curves for the MSP–AM powder were both nearly identical to those shown in Fig. 4.

The troughs in Fig. 4 correspond to the known behaviour and interactions of the powder constituents. Ammonium molybdate releases water of crystallization at 125 °C and

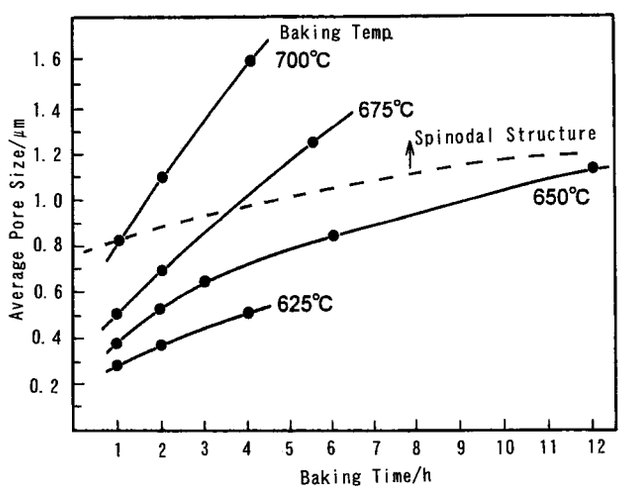

Fig. 2 Effects of baking temperature and baking time on pore size and silica structure, from the mixture used to prepare silica of 0.74 porosity; the dashed line represents the lower boundary for formation of the spinodal structure.

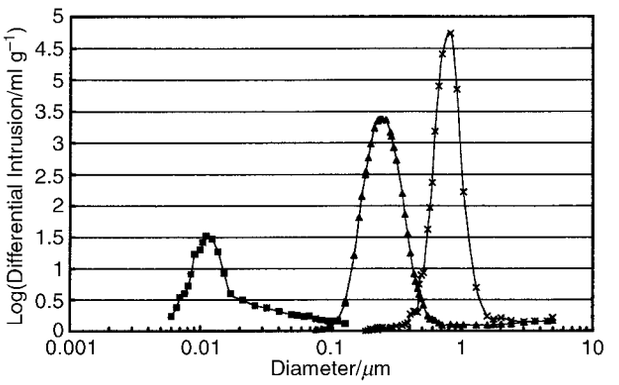

Fig. 3 Pore diameter and mercury intrusion of porous silicas obtained by baking for (■) 1 h at 350 °C, (▲) 15 min at 750 °C, and (×) 1 h at 750 °C.

generates ammonia and water at 200 °C due to its decomposition to molybdenum oxide. Under baking, monobasic sodium phosphate dehydrates to sodium oxide and diphosphorus pentaoxide, and, particularly where equimolar sodium and phosphorus are present (as was the case in the present study with monobasic sodium phosphate), these two oxides tend to form complex salts with molybdenum oxide which exhibit eutectic points of 550 °C to 750 °C or higher. Silica releases adsorbed water at about 150 °C. At 400 °C to 700 °C, the silanol groups at the silica surfaces undergo a condensation reaction, and silica surface dispersion occurs at about 800 °C.

This indicates that the broad heat absorption trough in Fig. 4 at about 100 °C is attributable to residual water evaporation, the trough at 310 °C to decomposition of ammonium molybdate by oxidation, the trough at 335 °C to decomposition of monobasic sodium phosphate by oxidation, and the trough at 610 °C to the eutectic point of the complex metal oxides of molybdenum with sodium and phosphorus from the phosphate oxidation reaction. It appears, also, that the broad trough at about 600 °C represents the eutectic point of other complex oxides formed in small amounts during the phosphate decomposition.

Porous silica composition

The baked porous silica powder was placed in water (one part powder in three parts water, by weight) at 80 °C for 1 h and then vacuum filtered with a 3G glass filter and dried, three times in succession. Fig. 5 shows the quantity of molybdenum (○) remaining in the porous silica, as determined by plasma luminescence, as a percentage of the total weight of the porous silica, after each washing, filtering, and drying cycle. These percentages are close to the values (△) predicted by calculating the quantity of molybdenum remaining in the porous silica at the end of each filtration based on the assumptions that (1) all

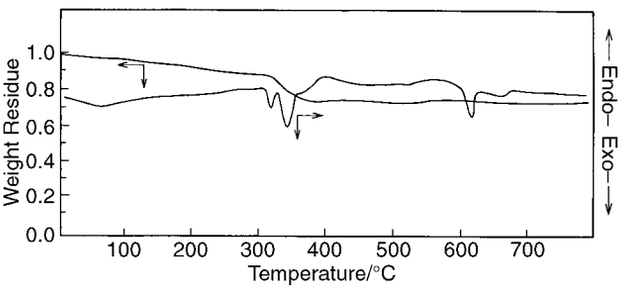

Fig. 4 Thermogravimetric (TG) and differential scanning calorimetric (DSC) curves of a powder obtained from a mixture of silica sol, monobasic sodium phosphate, and ammonium molybdate; temperature rise, 5 °C min^{-1}.

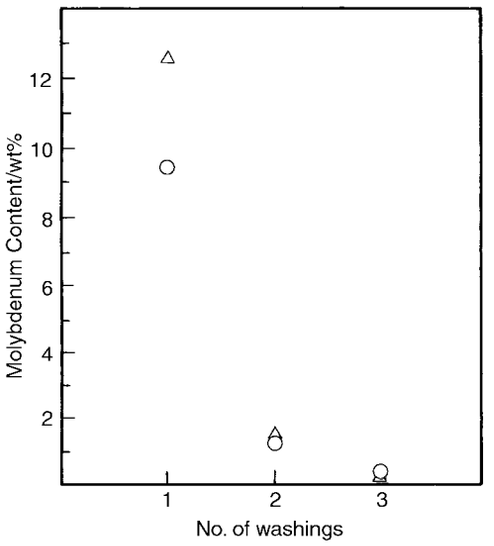

Fig. 5 Molybdenum content of porous silica powder after one, two, and three washings in water at 80 °C for 1 h; values obtained from measurement (○), and values predicted by calculation (△) under the assumption of complete dissolution of molybdenum-containing oxides and complete filling of pores by the resulting solution.

oxides containing molybdenum are completely dissolved in the water during washing and (2) the silica pores remain completely filled with the resulting solution after filtration. The agreement between the measured and calculated values indicates that the phosphates, nitrates, and molybdates which are added as salts to the silica form complexes, or heteropolyacids, which dissolve in a quantity of water about three times the weight of the silica powder.

As determined by plasma luminescence, the purity of the porous silica was 99.5% by weight after three cycles of washing and filtration, with the residual impurities consisting mainly of molybdenum and sodium.

Compressive strength

As shown in Table 2, the compressive strength, expressed as the compressive force at rupture, was measured for the porous spinodal silica with a porosity of 0.74, a shirasu porous glass with a porosity of 0.50, and a special-grade silica gel with a porosity of 0.68. For the first two, the compressive strength with a porosity of 0.68 was also calculated by extrapolation from the measured values, based on the relation between porosity and compressive strength as described by Nakashima *et al.* for phase-separated glasses.[9] The results indicate that the strength of the porous spinodal silica is about the same as that of shirasu porous glasses, and substantially higher than that of silica gels.

Mechanism of porous silica formation

As noted above, we found that the structure of the porous silica was spheroidal when baked at relatively low temperatures, but became spinodal, thus implying the occurrence of a spinodal separation mechanism, at higher temperatures. We investigated this further by varying the starting proportions of $NaPO_3$ and MoO_3 and the baking temperatures, and observing the resulting porous silica structures by SEM. The prevalence of spinodal microstructure in each porous silica was ranked from 1 (completely spheroidal, as shown in Fig. 1A) to 5 (completely spinodal, as shown in Fig. 1B), with the results shown in Fig. 6. Highly spinodal structures were obtained at 660 °C or higher with $NaPO_3$ contents (as molar ratios to MoO_3) of 20 to 35 mol%, and particularly at 680 °C with an $NaPO_3$ content of 30 mol%. As shown by comparison with the $NaPO_3$–MoO_3 phase diagram[10] in Fig. 7, the spinodal structure occurs most readily in the region where the $NaPO_3$ and MoO_3 coexist in the liquid state.

In the experimental results shown in Fig. 2, which were obtained with an $NaPO_3$ content of 36 mol%, the spinodal structure occurred at 675 °C, but not at 650 °C. This is also in agreement with the phase diagram of Fig. 7, which shows that for 36 mol% $NaPO_3$ the $NaPO_3$–MoO_3 mixture enters the fully molten phase at 670 °C. Fig. 2 shows further that the spinodal structure developed after about 1 h of baking at 700 °C, and after about 3.5 h of baking at 675 °C, and thus indicates that the speed of the spinodal structure development increases with increasing baking temperature.

As also shown in Fig. 2, the average pore size of the silica increased rapidly with increasing baking temperature for both the spinodal and the spheroidal structures, thus indicating rapid movement of the silica structure, and in this respect was therefore similar in behavior to phase-separated glass. In the production of such a glass, however, a homogeneously molten phase is obtained first by high-temperature fusion, and the temperature is then lowered to obtain phase separation. With the method used in the present study, in contrast, this fusion step is not employed and no homogeneously molten phase is attained. The porous silica thus clearly differs from phase-separated glass, in the mechanism of its development.

The results suggest, rather, that formation of the porous silica in the present study involves a mechanism of repeated decomposition and reformation, in which silica molecules are decomposed by the liquid $NaPO_3$–MoO_3 at the silica surface, and subsequently precipitate on the silica, lowering its surface energy. This cycle is constantly repeated, thus forming the porous silica structure.

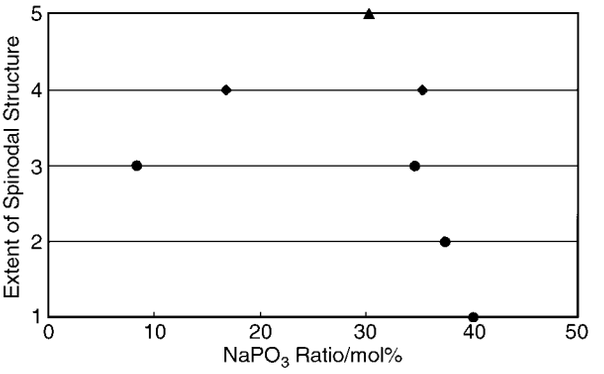

Fig. 6 Extent of spinodal structure on a scale of 1 (completely spheroidal) to 5 (completely spinodal), for porous silicas obtained from mixtures giving various ratios of $NaPO_3$ to MoO_3, after baking for 4 h at (●) 640 °C, (◆) 660 °C, and (▲) 680 °C.

Table 2 Compressive strengths of spinodal porous silica, in comparison with shirasu porous glass and silica gel

		Compressive force at rupture/kg cm^{-2}	
Granule structure	Porosity	Measured	Extrapolated to 0.68 porosity
Porous spinodal silica	0.74	132	158
Shirasu porous glass	0.50	370	164
Silica gel (special grade)	0.68	91	91

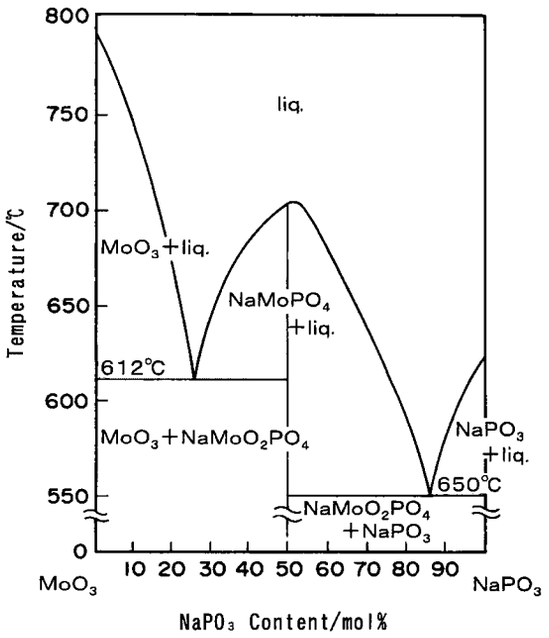

Fig. 7 Phase diagram of mixtures of $NaPO_3$ and MoO_3 in differing ratios.

The reasons for the narrow pore-size distribution which was obtained at high temperatures are not yet clear, but interaction between the silica and liquid $NaPO_3$–MoO_3 presumably also plays a major role in the formation of these highly uniform pore sizes.

Composite particles

Composite Aciplex‡ resin/silica particles with the desired level of ion exchange capacity were obtained, using the spinodal porous silica particles of 1.1 μm average pore size and 0.74 porosity, by repeating the impregnation procedure, in each repetition using only enough of the Aciplex resin solution to fill the silica particle pores so that the solution was completely drawn into the particle by capillary action and thus avoid the formation of a residual Aciplex coating on the particle surface which might desorb during use as a catalyst.

With the composite particles obtained in this manner, substantial desorption of the perfluoro ionomer from the particle pores was found to occur under immersion in acetone, methanol, and other polar organic solvents. We therefore heat-treated the composite particles, by first converting the implanted ionomer to the sulfonic soda state and then heating them to 250 °C for 1 h.

The effects of the heat treatment on the Aciplex resin/silica particles of two different exchange capacities and on commercially available Nafion resin/silica particles (SAC-13) were investigated by immersion of the particles in dimethyl formamide at 95 °C for 3 h, with the results shown in Table 3. The heat treatment resulted in lower ionomer desorption for all three composite particles. For the Aciplex resin/silica particles with ion exchange capacities of 0.37 and 0.51, as shown, the heat treatment lowered the ionomer desorption from 100% to 5% and from 100% to 70%, respectively. For these and other Aciplex resin/silica particles of various exchange capacities, it was found that the decrease in ionomer desorption generally became larger with decreasing exchange capacity. It is known that the tendency for perfluoro ionomers to crystallize generally increases with decreasing ion exchange capacity.[11] The results of these experiments therefore suggest that the decreased ionomer desorption was the result of crystallization in the ionomer network during the heat treatment, possibly as an effect of entanglement or other interaction between the main chains of the ionomer following the disruption of its micelles by heating.

As indicated by their pore-size distribution in Fig. 8, the average pore size of the Aciplex resin/silica particles was 0.7 μm, in contrast to the average pore size of 1.1 μm in the silica particles before their impregnation with the ionomer. In SEM micrographs of their cross section, such as that in Fig. 9, the ionomer network appears as convoluted strands of various thicknesses interwoven throughout the high-porosity spinodal silica network, which also suggests the occurrence of crystallization in the ionomer due to interaction between its constituent molecular chains. Further investigation will be necessary, however, to confirm both the crystallization and the related mechanism.

The heat treatment apparently had less effect on the SAC-13 composite particles. Their ionomer desorption with no heat treatment was 70%, in contrast to the 100% ionomer desorption by the untreated Aciplex resin/silica composites, but after heat treatment it was still 45%. The ion exchange capacity of the Nafion perfluoro ionomer in these particles is presumably 0.91 meq g^{-1}. With the Aciplex resin/silica particles of the same ion exchange capacity but presumably larger pore size and higher porosity, the heat treatment decreased the desorption from 100% to 5%. The smaller effect of heat treating on the SAC-13 may be attributable to a finely dispersed distribution of the ionomer in its silica network, due to the mixing of the ionomer with silica sol prior to the particle formation by gelation and hardening, resulting in relatively limited interaction between the ionomer chains during heat treatment, and less crystallization.

Catalytic activity

The catalytic activity of the Aciplex resin/silica composite particles for esterification of acetic acid is shown in Table 4, in comparison with those of Amberliste-15 and SAC-13 for the same reaction.

The reaction rate constant per functional group equivalent of the Aciplex resin/silica composite was 0.98 L mol^{-1} min^{-1} $eq(H^+)^{-1}$, which was about five times that of the Amberliste-15 resin (0.19 L mol^{-1} min^{-1} eq^{-1}) and about 1.4

‡Aciplex is a registered trademark of Asahi Chemical Industry Co., Ltd.

Table 3 Elution of perfluoro ionomer from composite particles with and without heat treatment, in dimethylformamide at 90 °C for 1 h, as determined by the change in ion exchange capacity

Perfluoro ionomer	Ion exchange capacity of ionomer/meq g^{-1}	Exchange capacity of composite/meq g^{-1}	Ionomer eluted (%)	
			Non-heat-treated composite	Heat-treated composite
Aciplex	0.91	0.37	100	5
Aciplex	1.10	0.51	100	70
SAC-13	N.A.[a]	0.16	70	45

[a]N.A.: Information not available.

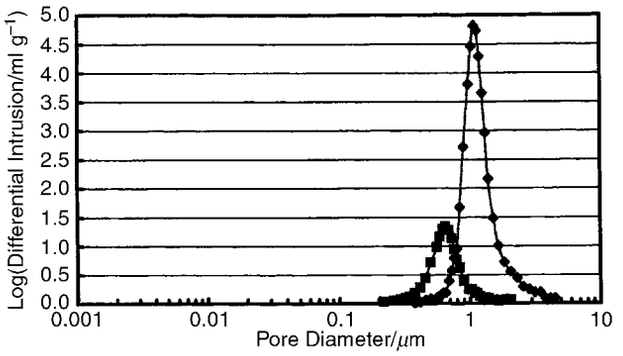

Fig. 8 Pore diameter and mercury intrusion of porous silica(◆) and Aciplex resin/silica (■).

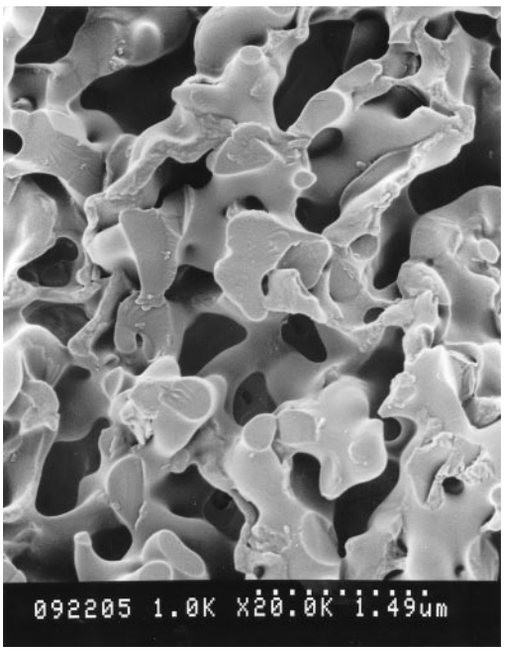

Fig. 9 Scanning electron micrograph of Aciplex resin/silica cross-section (× 20 000).

times that of the SAC-13 particles (0.70 L mol^{-1} min^{-1} eq(H$^+$)$^{-1}$). The low value obtained for the Amberliste-15 is attributable to the weak acidity of its benzene sulfonic acid, in comparison with the more strongly acidic perfluorosulfonic acid of the other two catalysts. The difference between the value obtained for the Aciplex resin/silica particles and that obtained for the SAC-13 particles, both of which employ perfluorosulfonic resins, is presumably attributable to the differing microstructures obtained by two fundamentally different particle production techniques.

By the impregnation of previously formed spinodal silica particles with the perfluoro ionomer, it was possible to obtain physically strong Aciplex resin/silica particles with an ion exchange capacity of 0.51 meq g^{-1}. This was only about one-tenth the ion exchange capacity of the Amberliste-15 resin (4.55 meq g^{-1}), but it was about three times as large as the ion exchange capacity of the SAC-13 particles (0.16 meq g^{-1}), which were obtained by the sol–gel technique. The reaction rate constant of the Aciplex resin/silica particles (0.50 L mol^{-1} min^{-1}) was 0.58 times that of Amberlist-15 (0.86 L mol^{-1} min^{-1}), because of the strong acidity of the perfluoro ionomer, and about 4.5 times that of the SAC-13 particles, because of the higher porosity and higher resin content of the Aciplex resin/silica particles.

Thermal stability

The Aciplex resin/silica particles were found to be physically and chemically stable at temperatures up to 200 °C or higher, which indicates that they may be useful as a practical catalytic system for a broad range of chemical reactions.

Conclusion

Previously unattainable spinodal silicas of high porosity can be obtained by baking a mixture of silica sol with sodium phosphate and molybdenum salts. Their structure is similar to that of spinodal phase-separated glasses, but the mechanism of their formation, and the range of their pore sizes and porosities as shown in Fig. 10, are clearly different from those of both silica gels and phase-separated glasses. Their predominantly spinodal structure is the result of repeated decomposition and precipitation of silica molecules at the silica surface in contact with molten $NaPO_3$–MoO_3, and the large size of the silica pores is also apparently an effect of interactions at this interface. Their composition was 99.5 wt% silica, and their compressive strength was far higher than that of silica gels despite their higher porosity.

Solid acid composites obtained by impregnating the high-porosity spinodal silica with perfluorosulfonic resin and heat treating can provide a combination of strong catalytic activity

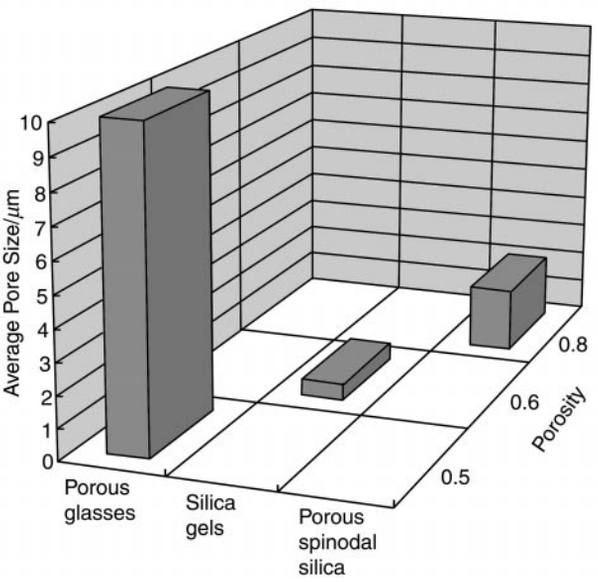

Fig. 10 Range of pore sizes and porosities obtained in the porous spinodal silica, in comparison with those generally obtainable in porous glasses and silica gels.

Table 4 Catalytic activity of Aciplex resin/silica composite particles, SAC-13 composite particles, and Amberliste-15 resin for esterification of acetic acid, in terms of exchange capacity per unit weight of catalyst system, reaction rate constant (k_1), and reaction rate constant per functional group equivalent (K)

Catalyst system	Catalyst system exchange capacity/meq g^{-1}	k_1/L mol^{-1} min^{-1}	K/L mol^{-1} min^{-1} eq(H$^+$)$^{-1}$
Aciplex resin/silica	0.51	0.50	0.98
Amberliste-15	4.55	0.86	0.19
SAC-13	0.16	0.11	0.70

and physical, chemical, and thermal stability, and therefore may be appropriate for a broad range of practical applications.

References

1 Japanese Unexamined Patent Publication No. 5817/1995.
2 H. P. Hood and M. E. Nordberg, Corning, New York, *US Pat.*, 2106744, 1934.
3 T. Nakashima and M. Shimizu, *Ceramics*, 1986, **21**, 408.
4 S. Omi, K. Katami, A. Yamamoto and M. Iso, *J. Appl. Polym. Sci.*, 1994, **51**, 1.
5 F. J. Waller and R. W. V. Scoyc, *Chemtech*, 1987, **17**, 438.
6 Y. Izumi, *Catal. Soc. Jpn.*, 1997, **39**, 292.
7 W. M. Van Rhijn, D. E. De Vos, B. F. Sels, W. D. Bossaert and P. A. Jacobs, *Chem. Commun.*, 1998, 317.
8 M. A. Harmer, W. E. Farneth and Q. Sun, *J. Am. Chem. Soc.*, 1996, **118**, 7708.
9 T. Nakashima, M. Shimizu and M. Kukizaki, *J. Ceram. Soc. Jpn.*, 1992, **100**, 1411.
10 A. G. Bergman and L. V. Semenyakova, *Zh. Neorg. Khim.*, 1970, **15**, 1386.
11 K. Okuyama and F. Nishikawa, *J. Chem. Soc. Jpn. Chem. Ind. Chem.*, 1994, **12**, 1091.

Paper a909620e